ISSN 1063-7834, Physics of the Solid State, 2015, Vol. 57, No. 10, pp. 2093–2098. © Pleiades Publishing, Ltd., 2015.
Original Russian Text © O.A. Ageev, A.P. Dostanko, E.G. Zamburg, B.G. Konoplev, V.V. Polyakov, D.I. Cherednichenko, 2015, published in Fizika Tverdogo Tela, 2015, Vol. 57, No. 10, pp. 2037–2042.

SURFACE PHYSICS AND THIN FILMS

Effect of the Processes in the Laser Ablation Plume on the Resistivity and Morphology of Nanocrystalline ZnO Films

O. A. Ageev[a], A. P. Dostanko[b], E. G. Zamburg[a, *], B. G. Konoplev[a], V. V. Polyakov[a], and D. I. Cherednichenko[a]

[a] *Institute of Nanotechnologies, Electronics, and Equipment Engineering, Southern Federal University, per. Nekrasovskii 44, Taganrog, 347928 Russia*

* *e-mail: zamburg.evgeniy@gmail.com*

[b] *Belarusian State University of Informatics and Radioelectronics, ul. P. Brovki 6, Minsk, 220013 Belarus*

Received January 22, 2015

Abstract—The specific features of the formation of nanocrystalline ZnO films by pulsed laser deposition have been studied at different target–substrate distances. Expressions for estimating the temperature, particle concentration, and pressure in the laser ablation plume have been obtained. The effect of these parameters on electrical properties of nanocrystalline ZnO films grown by pulsed laser deposition has been estimated. The feasibility of the controlled growth of nanocrystalline ZnO films with a surface roughness of ~2–15 nm, grain diameters of 70–620 nm, and resistivities in the range of $(1.75–5.3) \times 10^{-3}$ Ω cm has been demonstrated.

DOI: 10.1134/S1063783415100029

1. INTRODUCTION

Currently, promising nanoelectronic device structures have been fabricated widely using nanocrystalline ZnO films grown by pulsed laser deposition (PLD) [1]. Properties of nanocrystalline ZnO films depend strongly on deposition conditions, which allows their use in different nanoelectronic devices. For example, ZnO films with a fractal structure and high resistivity are necessary to fabricate sorption gas sensors; ZnO films with different conductivity, high carrier concentrations and mobilities are claimed as transparent conductive coatings, functional layers of diode and transistor structures of nanoelectronics, devices of spintronics, and piezoelectric devices [1–3].

The laser ablation theory was developed for the laser effect of the surface of monatomic materials. However, since the laser ablation is a high-temperature process, it is reasonable to expect that laser irradiation of a complex-composition target can cause dissociation of target material molecules; therefore, the structure, composition, and properties of films grown by laser ablation during pulsed laser deposition of target materials can differ. Nonetheless, little attention has been paid to stoichiometry retention in published studies, since it has been believed that the incongruence effect in complex-composition target evaporation upon laser exposure has no time to manifest itself.

The application of existing theories to quantitatively estimate the processes of complex-composition film growth by the PLD method faces significant difficulties. However, using the ablation surface temperature and velocity as additional parameters for formulating boundary conditions at the plume base and taking into account the self-similarity of the polytropic plume expansion [4], we can obtain analytical relations defining the thermodynamic state of the plume as applied to laser ablation as the method for fabricating nanostructured materials for nanoelectronic device structures.

2. ABLATION SURFACE TEMPERATURE AND VELOCITY

According to the thermal ablation theory, the ablation surface temperature in the laser radiation power density range of $10^6–10^9$ W/cm^2 is determined from the transcendental equation [4]

$$\frac{\rho_M c}{Q} = \frac{\exp(L_b/RT^*)}{(L_b + 2.5RT^*)}, \quad (1)$$

where $\rho_M = \rho/M$ is the molar density, ρ is the specific density of a target material, M is the molecular mass of a target material, Q is the specific power of laser radiation absorbed by the target surface, $c = (E/\rho)^{1/2}$ is the speed of sound, E is Young's modulus, L_b is the molar latent sublimation heat, R is the universal gas constant, and T^* is the ablation surface temperature.

Therefore, the difference between the ablation process and the surface evaporation process with close mathematical formulation becomes evident. During surface evaporation, the body surface temperature is assumed to be given and equal to the boiling temperature T_m, while the temperature T^* during ablation depends on the flux density q and is determined from expression (1).

Using the heat balance condition on the laser radiation absorption surface, it was shown [4] that the ablation surface velocity also depends on the laser beam power, and it can be determined at the known ablation surface temperature,

$$V_0 = \frac{Q}{\rho_M(L_b + 2.5RT^*)}. \quad (2)$$

As a result, the flux density of atoms sublimated from unit area of the ablation surface per unit time can be estimated by the formula

$$F_0 = V_0 n_0, \quad (3)$$

where $n_0 = \rho N_A/M$ is the number of atoms per unit volume of the target material and N_A is Avogadro's number.

3. PLUME PROCESSES, FREE EXPANSION MECHANISM

The laser ablation process is accompanied by the rapid material removal from the exposed area and the formation of the rapidly expanding plume heated to a high temperature. The motion in the plume is considered as self-similar expansion of a polytropic ideal gas [4]. This process is a specific type of unsteady motion during which the distributions of the particle concentration, gas pressure and temperatures in the flux depend on the spatial coordinate x and time t in the form of a single parameter with the velocity dimension $\xi = x/t$ [5].

Using the self-similar variable ξ, the entropy conservation equation

$$\frac{\partial s}{\partial t} + V\frac{\partial s}{\partial x} = 0 \quad (4)$$

can be reduced to the form

$$(V - \xi)\frac{\partial s}{\partial \xi} = 0. \quad (5)$$

Since the particle velocity V in flux and the variable ξ are nonzero, the derivative of the entropy determines the meaning of equality (5). Hence, it follows that the entropy s in the system is constant, and the one-dimensional self-similar motion is adiabatic.

Similarly, transforming the Euler equations using the self-similar variable ξ, it can be shown that the velocity in the case free expansion of the flow of particles sublimated by ablation is given by [6]

$$u = \frac{V}{V_m} = \alpha + (1 - \alpha)\xi, \quad (6)$$

where

$$V_m = \frac{2c_0}{\gamma - 1} \quad (7)$$

is the maximum front velocity during free flow expansion, and

$$c_0 = \left(\gamma\frac{RT}{m}\right)^{\frac{1}{2}} \quad (8)$$

is the speed of sound in the immobile gas, γ is the polytropic exponent, the parameter $\alpha = (\gamma - 1)/(\gamma + 1)$ is within $1 \geq \alpha \geq 0$, and $\xi = \xi/V_m$ is the dimensionless self-similar variable.

4. ENHANCED EXPANSION MECHANISM

In contrast to the free expansion mechanism, the enhanced expansion mechanism takes into account the continuous energy and material supply to the plume from the ablation surface during laser pulse. Assuming that the plume expands in vacuum, the boundary conditions for the particle concentration, velocity and temperature at the plume leading edge can be written as

$$n = 0, \quad V = V_m, \quad T = 0 \quad (9)$$

at $\xi = 1$.

As the second condition, we use the law of conservation of matter

$$n_0 = V_0 = V_m\int_0^1 n(\xi)d\xi. \quad (10)$$

Therefore, it is obvious that boundary condition (9) at the plume leading edge is satisfied by the self-similar motion velocity u (6).

A detailed description of the factors acting in the region adjacent to the ablation surface is given in [4, 6]. It was assumed that the plume rear edge and the ablation surface coincide (at $x = 0$). As the laser is turned on at the time point $t = 0$, the particle flux energy in the plume is sufficient to enhance motion of sublimated atoms in the plume. It was assumed that the plume vapor pressure and viscosity at a moderate exposure power ($q \leq 10^9$ W/m^2) allow us to consider the gas to be ideal; in this case, the beam energy loss and ionization of atoms in vapor can be neglected. It was also accepted that the Knudsen effect slightly affect the ablation process, and the atomic velocity at the evaporation surface was set to zero ($V = 0$). Since the speed of sound is much higher than the ablation surface velocity, $c_0 \gg V_0$, the effect of the ablation surface velocity on the plume expansion velocity can also be neglected. In this case, the vapor pressure in the plume is calculated by the known formula of the kinetic theory of gases,

$$P = nkT. \quad (11)$$

Taking into account these assumptions, in solving the problem, as in [5], we use the law of conservation of matter and energy; as additional conditions, we con-

sider the ablation surface temperature and velocity to be known, i.e., determined by formulas (1) and (2) according to the thermal ablation theory [4].

In what follows, this makes it possible to significantly facilitate the determination of integration constants and the calculation of technological process parameters.

To study the dynamics of transport processes in the plume, the Euler equations are used,

$$\frac{\partial n}{\partial t} = -\frac{\partial (nV)}{\partial x}, \tag{12}$$

$$m\frac{\partial (nV)}{\partial t} = -\frac{\partial}{\partial x}\left(P + \frac{mnV^2}{2}\right). \tag{13}$$

Using the self-similar variable, Eqs. (12) and (13) are transformed to the form

$$\frac{\partial n}{\partial \xi} = -\frac{n}{u-\xi}\frac{\partial u}{\partial \xi}, \tag{14}$$

$$\frac{\partial P}{\partial \xi} = -\left[mnV_m^2(1-\xi)\alpha\frac{\partial u}{\partial \xi}\right]. \tag{15}$$

To determine the distribution of the particle concentration in the plume, we substitute the reduced velocity from Eq. (6) into (14) and, integrating, we obtain

$$n = A(1-\xi)^{\frac{1-\alpha}{\alpha}}. \tag{16}$$

Then, determining the integration constant on the basis of the law of conservation of matter

$$n_0V_0 = AV_m\int_0^1(1-\xi)^{\frac{1-\alpha}{\alpha}}d\xi, \tag{17}$$

for calculating the particle concentration profile in the plume, we obtain

$$n(\xi) = \frac{n_0V_0}{\alpha V_m}(1-\xi)^{\frac{1-\alpha}{\alpha}}. \tag{18}$$

Then, substituting the obtained relation for the particle concentration into Eq. (15) and integrating taking into account the reduced velocity, we obtain the pressure distribution in the plume in the form

$$P(\xi) = mn_0V_0V_m\alpha\frac{(1-\alpha)}{(1+\alpha)}(1-\xi)^{\frac{1+\alpha}{\alpha}}. \tag{19}$$

To calculate the temperature profile, we used relation (11) and relations for the particle concentration and pressure in the plume (18) and (19). As a result of the substitution of the concentration and pressure P into relation (11), we obtain

$$T(\xi) = \frac{mV_m^2}{k}\alpha^2\frac{(1-\alpha)}{1+\alpha}(1-\xi)^2. \tag{20}$$

During polytropic expansion, the energy of sublimated particles in vapor at the interface with the ablation surface will be given by (at $\xi = 0$)

$$E_0 = \frac{n_0V_0kT^*}{\gamma-1}, \tag{21}$$

and the energy conservation law can be written as

$$\int_0^1 E_0dt = \int_0^X Edx, \tag{22}$$

where X is the particle drift space during plume expansion.

Defining the energy in the expanding plume as the sum of the potential and kinetic energies,

$$E = \frac{nkT}{\gamma-1} + \frac{mnV^2}{2} \tag{23}$$

and transforming Eq. (22) using the self-similar variable, we obtain

$$E_0t = V_mt\int_0^1\left(\frac{nkT}{\gamma-1} + \frac{mnV^2}{2}\right)d\xi. \tag{24}$$

Substituting the formulas for the particle temperature, concentration, and velocity in the plume (18)–(20) into the integrand in Eq. (24), we can obtain the relation for the maximum velocity of the plume edge during enhanced expansion,

$$V_m = \left[\theta\frac{kT^*}{m}\right]^{\frac{1}{2}}, \tag{25}$$

where

$$\theta = \frac{(1+\alpha)^2(2\alpha+1)}{\alpha(1-\alpha)[\alpha+\alpha^2+\beta(5+\alpha^3+\alpha^4)]},$$

$$\beta = \left[\frac{(\gamma-1)(1+\alpha)}{2\alpha(1-\alpha)}\right].$$

The work done during an increase in the plume volume in the one-dimensional expansion approximation can be estimated as

$$\Delta W = \frac{R}{1-\gamma}(T^* - T). \tag{26}$$

Since the polytropic exponent is $\gamma > 1$, equality (26) is in fact a change in the Gibbs free energy accumulated by the plume upon the material ejection during the laser pulse. Taking into account the adiabaticity of self-similar expansion, it can be concluded that the entire free energy store is expended to enhance plume processes with increasing volume. It should also be

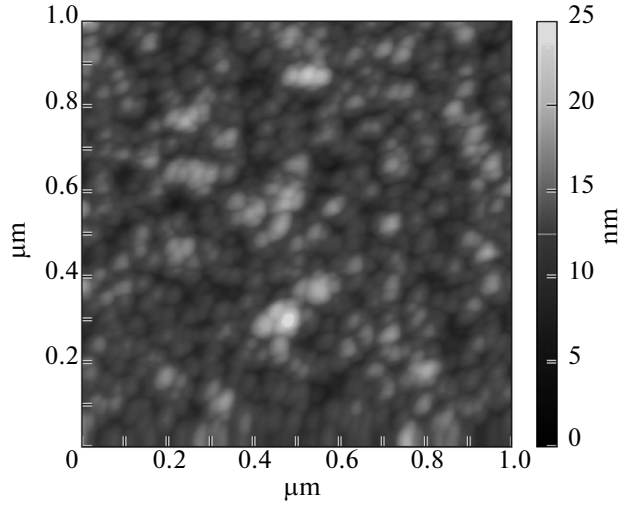

Fig. 1. Atomic force microscopy image of the ZnO film at a target–substrate distance of 135 mm.

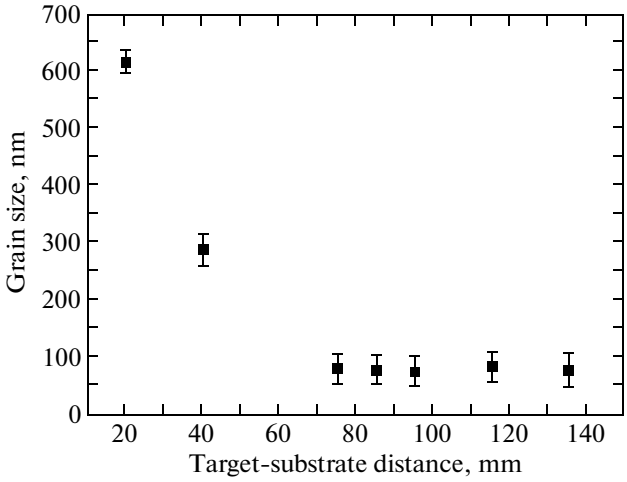

Fig. 2. Dependence of the grain diameter of ZnO films on the target–substrate distance.

noted that the boundary condition for the temperature of the target–plume interface plane

$$T = T^*|_{\xi(x) = 0}$$

is satisfied only at the polytropic exponent $\gamma = 1.5907$. This polytropic exponent determined in the calculation is close to the value determined for polytropic expansion of a monatomic flow.

5. EXPERIMENT

Zinc oxide films were grown in a PLD module (Neocera, United States) incorporated in a NANOFAB NTK-9 cluster nanotechnological system (NT-MDT, Russia) [7, 8]. The film morphology was studied using an Ntegra probe nanolaboratory (NT-MDT, Russia). Electrical parameters of ZnO films were determined by the Hall emf method using an Ecopia HMS-3000 system.

Glass ceramics with preliminarily chemically cleaned surface was used as a substrate material. ZnO films were grown at a substrate temperature of 300°C and a carrier gas (oxygen) pressure of 1×10^{-3} Torr in the chamber. The films were grown at a target–substrate distance varied in the range of 20–135 mm.

6. EXPERIMENTAL RESULTS

The atomic force microscopy (AFM) image of the film surface is shown in Fig. 1.

The dependences of the grain diameter and resistivity of ZnO films on the target–substrate distance are shown in Figs. 2 and 3.

The results shown in Figs. 1–3 suggest that the thermal conditions of film growth at different target–substrate distances significantly affect not only the structure, but also electrical properties of films.

7. NUMERICAL ANALYSIS OF THE RESULTS

To calculate the laser ablation parameters, i.e., the target surface temperature T^* and the ablation surface velocity V_0, we should know the latent sublimation heat of a material. The ZnO latent sublimation heat was estimated using the molecule dissociation enthalpy

$$L_b = \Delta H_T^0 + (RT)/2. \quad (27)$$

The temperature at which the dissociation reaction ZnO(cryst) ⟷ Zn(gas) + O(gas) occurs was determined by the conventional method using the change

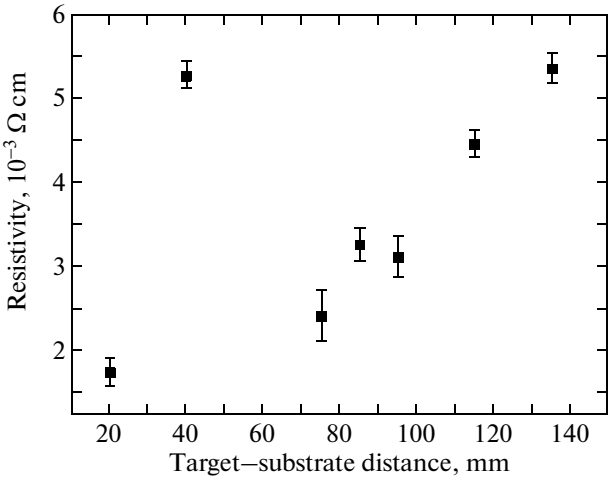

Fig. 3. Dependence of the resistivity of the ZnO film on the target–substrate distance.

in the Gibbs free energy. Using the standard thermodynamic constants of initial substances and reaction products [9], the Kirchhoff equations for calculating the enthalpy and entropy, and PLD technological parameters, it can be shown that a change in the Gibbs potential of the ZnO dissociation reaction at T_d = 2594 K becomes negative, $\Delta G_T^0 = -30.545$ J/mol. On the basis, the temperature T_d is taken as the starting point of ZnO dissociation as the target surface temperature increases upon laser exposure. The dissociation enthalpy at this point is $\Delta H_T^0 = 7.356 \times 10^5$ J/mol; according to Eq. (27), the latent sublimation heat is $L_b = 7.464 \times 10^5$ J/mol.

According to model (1)–(26), for ZnO film growth conditions described in this paper, at the exposure power $Q = 1.333 \times 10^9$ J/(m^2 s), the ablation surface temperature is $T^* = 7720$ K and the ablation surface velocity is $V_0 = 0.021$ m/s. The maximum plume front velocity during enhanced expansion, according to Eq. (25), is $V_m = 4.912 \times 10^3$ m/s. The particle velocity at different stages of plume expansion is

$$V = \xi V_m. \quad (28)$$

For the spatial representation of the particle velocity at the target–substrate distance in the real coordinate system, the self-similar coordinate ξ was transformed according to the criterion relation

$$K = \frac{x\tau}{tX\xi} = 1, \quad (29)$$

where τ is the transit time.

The temperature distribution along the longitudinal plume axis, calculated according to model (1)–(26), is shown in Fig. 4.

We can see that the plume temperature at the target–substrate distance $0 < x < 0.057$ m significantly exceeds the ZnO dissociation temperature. In this significantly overheated region, additional sublimation of flying fragments of target material will occur, whose intensity depends on the distance, as indicated by the decrease in the grain diameter in the film structure formed at these distances. The decrease in the film resistivity also indicates an increase in the metal zinc fraction in the film component composition (Figs. 2–4).

The size factor [10] also has a significant effect on electrical properties of nanostructured films, which consist in that the object surface-to-volume ratio $\omega = S_c/v_c$ increases in going to small sizes. This value appears higher than that in the case of macroscopic objects by many orders of magnitude. For grains formed at target–substrate distances $0 < x \le 0.057$ m, ω increases from 9.6×10^6 to 2.069×10^7 cm^{-1} with increasing distance due to additional ZnO dissociation. At target–substrate distances $x > 0.057$ m, when the plume temperature becomes below the ZnO dissociation temperature, the value of ω remains almost unchanged (7.595×10^7–7.947×10^7 cm^{-1}). The individual grain resistance can be estimated by the expression $R_c = \rho_c\omega$ [Ω]. To estimate the film resistance and to determine its physical nature, we can use the expression

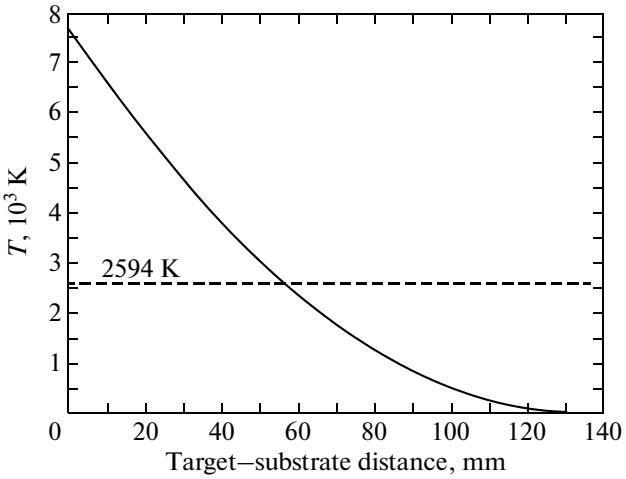

Fig. 4. Dependence of the plume temperature on the target–substrate distance.

$$R_c = \rho_c\omega\beta_v d_c, \quad (30)$$

which includes the individual grain resistance, the configuration factor β_v, and the grain diameter d_c.

For the film, the configuration factor is $\beta_v = l/(bh)$, where l and b are the longitudinal and transverse film sizes, and h is the film thickness. At such size factors and feature film sizes $l = 1.0$ cm and $b = 1.0$ cm and $h = 50$ nm, the resistivities are 1.969×10^5–9.137×10^4 Ω and 2.426×10^4–2.379×10^4 Ω at target–substrate distances $0 < x \le 0.057$ m and $x > 0.057$ m.

We can see from Eq. (30) that the resistance of films grown at target–substrate distances $x \le 0.057$ m is determined by the resistivity (the component composition of the film material), the size factor, and grain diameter. The resistance of films grown at target–substrate distances $x > 0.057$ m, at which thermal conditions are favorable for reverse chemical reactions, is determined only by the material component composition. If we take into account that the room-temperature zinc and zinc oxide resistivities are 5.92×10^{-6} Ωcm [9] and 10^8 Ω cm [11], then, according to experimental data (Figs. 3 and 4), the decrease in the grain size during dissociation is accompanied by the increase in the pure zinc fraction at the target–substrate distance $x \le 0.057$ m. At the target–substrate distance $x > 0.057$ m and the constant size factor, the increase in the resistivity is caused by the increase in the ZnO fraction in the film structure. The fact that the size factor in this plume region remains constant and the film component composition rapidly varies allows the conclusion that the chemical transforma-

tion rate significantly exceeds the cluster size evolution rate in the plume.

8. CONCLUSIONS

A technique for estimating the parameters of the nanocrystalline ZnO film growth by pulsed laser deposition was proposed. It was shown that laser ablation of complex materials is characterized by rapid dissociation of target material molecules. In the initial plume region, in which the temperature significantly exceeds the ZnO dissociation temperature, additional sublimation of target material clusters, is observed. In the region where the plume temperature becomes lower than the ZnO dissociation temperature, reverse chemical reactions take place. It was found that ZnO films grown at different target–substrate distances have different structures and substantially different electrical properties.

The capabilities of laser ablation as a technological method for growing nanocrystalline ZnO films for different functionalities in devices of nanoelectronics and nanosystem engineering are demonstrated.

ACKNOWLEDGMENTS

The authors are grateful to A.V. Shumov, Z.E. Vakulov, and D.E. Vakulov for their assistance in measurements, calculations, and paper preparation.

This study was supported by the Russian Foundation for Basic Research (project no. 14-08-90010 Bel_a), Belarusian Republican Foundation for Basic Research (project no. T14R-165), and project part of the State task in the scientific activity sphere (task no. 16.1154.2014/K).

The results were obtained using the equipment of the Shared Service Center and the "Nanotechnology" Science and Education Center of the Southern Federal University.

REFERENCES

1. H. Morkoc and U. Ozgur, *Zinc Oxide Fundamentals, Materials and Device Technology* (Wiley, Weinheim, 2009).
2. E. G. Zamburg, O. A. Ageev, E. Y. Gusev, D. E. Vakulov, Z. E. Vakulov, A. V. Shumov, and M. N. Ivonin, Appl. Mech. Mater. **475–476**, 446 (2014).
3. A. P. Dostanko, O. A. Ageev, D. A. Golosov, S. M. Zavadskii, E. G. Zamburg, D. E. Vakulov, and Z. E. Vakulov, Semiconductors **48** (9), 1242 (2014).
4. S. I. Anisimov, Ya. A. Imas, G. S. Romanov, and Yu. V. Khodyko, *Action of High-Power Radiation on Metals* (Nauka, Moscow, 1970; Consultants Bureau, Springfield, Virginia, 1971).
5. L. D. Landau and E. M. Lifshitz, *Course of Theoretical Physics*, Vol. 6: *Fluid Mechanics* (Gostekhizdat, Moscow, 1954; Pergamon, London, 1959).
6. K. R. Chen and J. N. Leboeuf, J. Vac. Sci. Technol., A **14** (3), 5 (1996).
7. O. A. Ageev, A. S. Kolomiitsev, A. V. Mikhailichenko, V. A. Smirnov, V. V. Ptashnik, M. S. Solodovnik, A. A. Fedotov, E. G. Zamburg, V. S. Klimin, O. I. Il'in, A. L. Gromov, and A. V. Rukomoikin, Izv. Yuzhn. Fed. Univ., Tekh. Nauki **114** (1), 109 (2011).
8. O. A. Ageev, D. A. Golosov, E. G. Zamburg, A. M. Alexeev, D. E. Vakulov, Z. E. Vakulov, A. V. Shumov, and M. N. Ivonin, Appl. Mech. Mater. **481**, 55 (2014).
9. *Tables of Physical Quantities*, Ed. by I. K. Kikoin (Atomizdat, Moscow, 1976; Mir, Moscow, 1978).
10. J. Frenkel, *Kinetic Theory of Liquids* (Dover, New York, 1955; Nauka, Leningrad, 1975).
11. Yu. V. Koritskii, V. V. Pasynkov, and B. M. Tareev, *Handbook on Electrotechnical Materials* (Energoatomizdat, Leningrad, 1988) [in Russian].

Translated by A. Kazantsev